Dermatan Sulfate Epimerase 1 Deficient Mice as a Model for Human Abdominal Wall Defects

Renata Gustafsson*[1], Xanthi Stachtea[2], Marco Maccarana[2], Emma Grottling[3], Erik Eklund[4], Anders Malmström[2], and Åke Oldberg[5]

Background: Dermatan sulfate (DS) is a highly sulfated polysaccharide with a variety of biological functions in extracellular matrix organization and processes such as tumorigenesis and wound healing. A distinct feature of DS is the presence of iduronic acid, produced by the two enzymes, DS-epimerase 1 and 2, which are encoded by *Dse* and *Dsel*, respectively. **Methods:** We have previously shown that *Dse* knockout (KO) mice in a mixed C57BL/6–129/SvJ background have an altered collagen matrix structure in skin. In the current work we studied *Dse* KO mice in a pure NFR genetic background. **Results:** *Dse* KO embryos and newborns had kinked tails and histological staining revealed significantly thicker epidermal layers in *Dse* KO mice when compared with heterozygote (Het) or wild-type (WT) littermates. Immunochemical analysis of the epidermal layers in newborn pups showed increased expression of keratin 5 in the basal layer and keratin 1 in the spinous layer. In addition, we observed an abdominal wall defect with herniated intestines in 16% of the *Dse* KO embryos. Other, less frequent, developmental defects were exencephaly and spina bifida. **Conclusion:** We conclude that the combination of defective collagen structure in the dermis and imbalanced keratinocyte maturation could be responsible for the observed developmental defects in *Dse* KO mice. In addition, we propose that *Dse* KO mice could be used as a model in pathogenetic studies of human fetal abdominal wall defects.

Birth Defects Research (Part A) 100:712–720, 2014.

Key words: abdominal wall defect; neural tube defects; embryonic development; dermatan sulfate epimerase 1; epidermis

Introduction

Proteoglycans (PGs) consist of a core protein with covalently attached glycosaminoglycan chains (GAGs). The PGs form large, complex structures in the extracellular connective tissue and play role in a wide variety of biological processes, including embryonic development, wound healing, cell proliferation and migration, growth factor binding and extracellular matrix organization (Bulow and Hobert, 2006; Esko et al., 2009). One GAG family includes chondroitin sulfate (CS) and dermatan sulfate (DS), the latter distinguished by the presence of iduronic acid (IdoA) (Thelin et al., 2013). IdoA, which is the C-5 epimer of D-glucuronic acid, occurs in variable amounts in DS and makes the DS chains more flexible (Thelin et al., 2013). DS-PGs include the small leucin-rich PGs decorin, biglycan and members from the lectican family such as versican (Malmstrom et al., 2012). The formation of DS requires the enzymes dermatan sulfate epimerase 1 (DS-epi1, encoded by *Dse*), dermatan sulfate epimerase 2 (DS-epi2, encoded by *Dsel*) and DS-4-O-sulfotransferase 1 (encoded by *D4st1*). Several studies have been undertaken to elucidate the function of DS. We have shown that mice deficient in DS-epi1 were viable in a mixed C57BL/6–129/SvJ genetic background, and their skin was more fragile due to altered collagen fibril morphology compared with their WT littermates (Maccarana et al., 2009), thus demonstrating the importance of IdoA in skin development. In addition, mutations in the human *DSE* and *D4ST1* genes result in subtypes of Ehlers-Danlos syndrome (Miyake et al., 2010; Muller et al., 2013). DS-epi1 is the major contributor of epimerase activity, and mice deficient in DS-epi2 do not display any significant defects (Bartolini et al., 2012), thus showing that DS-epi1 is able to compensate for the absence of DS-epi2 in most tissues except for the brain (Bartolini et al., 2012).

Because earlier experiments during the generation of the DS-epi1 KO mice in pure C57BL/6 genetic background indicated a high frequency of perinatal lethality, mice from the mixed C57BL/6–129/SvJ genetic background were back-crossed into mice with pure NFR genetic background. The NFR strain is an albino Swiss mouse originating from an inbred NMRI mouse strain developed and maintained at the National Institute of Health (Bethesda, MD).

[1]Department of Experimental Medical Science, BMC D10, Lund University, Lund, Sweden
[2]Department of Experimental Medical Science, BMC D12, Lund University, Lund, Sweden
[3]Section for Child Surgery, Lund University, Lund, Sweden
[4]Clinical Sciences, Section for Pediatrics, BMC D12; Lund University, Lund, Sweden
[5]Department of Experimental Medical Science, BMC B12. Lund University, Lund, Sweden.

Additional Supporting Information may be found in the online version of this article.

This work was funded by Cancerfonden (to M. Maccarana, no.130388), the Swedish Research Council (to A. Malmström, no. 2012–2631; to Å. Oldberg, no. 2013–7478), the Medical Faculty of Lund University (to A. Malmström), the Mizutani Foundation (to M. Maccarana, no. 120115), the Albert Österlund Foundation (to A. Malmström and Å. Oldberg), the Greta and Johan Kock Foundation (to A. Malmström and Å. Oldberg), and the Anna-Greta Crafoord Foundation (to A. Malmström).

*Correspondence to: Renata Gustafsson, Lund University, Experimental Medical Science, BMC D10, 221 84, Lund, Sweden.
E-mail: renata.gustafsson@med.lu.se

Published online 4 September 2014 in Wiley Online Library (wileyonlinelibrary.com). Doi: 10.1002/bdra.23300

We chose the NFR strain because the females are known to produce large litters (Liljander et al., 2009).

The aim of the current study was to elucidate if DS-epi1 deficiency causes early embryonic developmental defects.

Materials and Methods

ETHICS STATEMENT

All animal experiments were approved by the ethical committee for animal experiments in Lund, Sweden (permit number: M164-10).

MICE

Mice deficient in DS-epi1 in the mixed C57BL/6–129/SvJ genetic background (Maccarana et al., 2009) were back-crossed with mice in pure C57BL/6 or NFR background (the later kindly provided by Prof. Ragnar Matsson, Lund University, Sweden) for more than 10 generations. Het and KO mice in NFR background were mated to obtain a high ratio of the *Dse* KO genotype. In addition, *Dse* Het/Het mice were mated to obtain WT, *Dse* Het and KO newborn pups (one litter). Time-mated pregnant *Dse* Het females were euthanized and embryos from embryonic day E13.5 to E18.5 and newborn pups were harvested and body weight was measured. Mice were genotyped by PCR on extracted DNA from tail (mothers) or yolk sac (embryos and newborn) with the following primers: forward primer for both alleles, 5′-AGCACATTGCAGCTCGGCTTAC-3′; reverse primer for the wild-type allele, 5′-GCTGCCATCCTC TCCATGTAGTC-3′; reverse primer for the neomycin cassette-mutated allele, 5′-TGGATGTGGAATGTGTGCGAGG-3′.

MORPHOLOGICAL ANALYSIS

Embryos at stages E13.5, E16.5, E18.5, and tails from newborn pups were washed in ice cold PBS and immersed in HistoChoice tissue fixative (Amresco Inc). Embryos and newborn tails were fixed for 2 days (E13.5, E16.5, and tails) or 5 days (E18.5). After fixation tissues were rinsed in PBS, dehydrated in a series of rising ethanol concentrations, two changes of xylene, paraffin overnight, then embedded in paraffin and serially sectioned (5 μm). For histological assessment, Masson's trichrome staining of whole embryonic sections was performed using the "Accustain trichrome stain (Masson)" (Sigma-Aldrich) according to the manufacturer's instructions. Stained sections were scanned and digitalized using an Aperio ScanScope digital slide scanner (Scanscope Console v8.2. 0.1263, Aperio Technologies, Inc., Vista, CA).

For morphological measurements on *Dse* Het and KO embryonic epidermis, 2 to 5 consecutive sagittal sections from E13.5, E16.5, and E18.5 embryos were analyzed by measuring the epidermis from stratum basale to stratum corneum around the whole embryonic section with approximately 70-μm intervals (up to 130 measurements per section were performed). For morphological measurements on WT, *Dse* Het and KO tail epidermal thickness ($n = 3$ for each genotype), transverse sections from 3 different locations (at least 100 μm apart) were measured around the tail epidermis with approximately 70-μm intervals between measurement points and up to 70 measurements per tail section.

IMMUNOFLUORESCENCE STAINING

Paraffin sections from WT, *Dse* Het, and KO tails from 3 different locations ($n = 3$ for each genotype) were rehydrated in decreasing ethanol concentrations and rinsed in PBS. Sections were blocked in 1.5% goat serum and 0.05% Tween/PBS for 1 hr and incubated with primary antibodies (all from Abcam) produced in rabbit against keratin 1 (dilution 1:1000; ab24643), keratin 5 (dilution 1:1000; ab24647), loricrin (dilution 1:200; ab24722), and Ki67 (dilution 1:200; ab16667) overnight at +4°C. Next, sections were rinsed in PBS and incubated with anti-rabbit secondary antibodies produced in goat (dilution 1:200; Alexa Fluor® 488; A11008; Invitrogen), for 2 hr. After incubation, sections were rinsed, dehydrated in increasing concentrations of ethanol and dipped in xylene. Slides were mounted with Vectamount containing DAPI (Vector Labs), and staining was visualized using a Nikon Eclipse 80i microscope (Nikon Instruments, Japan). Ki67 immunolabeling for proliferation in the epidermal layers ($n = 3$ for each genotype) was analyzed by ImageJ software using the "Analyze Particles" function.

WESTERN BLOT

Whole body skin (dermis and epidermis) were harvested from newborn WT, *Dse* Het and KO pups ($n = 3$ per genotype). Samples (60–100 mg) were homogenized using a Potter-Elvehjem homogenizer on ice in 10 volumes of extraction buffer (Tris 50 mM, pH 7.4, 150 mM NaCl, 1 mM EDTA, 1% DOC, 1% NP-40, 1% SDS, 1 mM DTT, protease inhibitors from Roche, 1mM PMSF), and an equal amount of protein (6 μg per well) was loaded and run on 10% SDS-PAGE. The gels were transferred to PVDF membrane (Hybond™-P, Amersham) and probed first with the primary antibodies against keratin 1 or keratin 5 (dilution 1:3000, ab24643, and ab24647, respectively; Abcam) and Gapdh (dilution 1:2000, sc47724; Santa Cruz) and then with the secondary antibody conjugated with horseradish peroxidase (dilution 1:4000, goat anti-rabbit IgG-HRP, sc2004, Santa Cruz). Signals were detected using ECL Plus detection system (Amersham) according to the manufacturer's instructions and analyzed in ImageJ software (NIH, Bethesda, MD).

STATISTICAL ANALYSES

Statistical analysis on embryonic epidermal thickness was analyzed using two-way ANOVA with time and genotype as factors. Analysis was performed in SPSS software version 21 (IBM Corporation, Somers, NY). Statistical analysis on tail epidermal thickness and results from ImageJ analysis were performed on GraphPad Prism Version 6.0 using Student's *t* test or one-way ANOVA analysis with Tukey's

TABLE 1. *Genotypes and Mendelian ratios*

Background	Genotype/Mating	Age	Mice no.	Dse WT	Dse Het	Dse KO
C57BL/6	Het/Het	E14.5 - E15.5	46	8 (17%)	23 (50%)	15 (33%)
C57BL/6	Het/Het	Newborn	51	16 (31%)	28 (55%)	7 (14%)[a]
C57BL/6	Het/Het	Weaning	72	24 (33%)	48 (67%)	0
NFR	Het/KO	E13.5 - Newborn	143[b]	-	69 (48%)	74 (52%)
NFR	Het/Het	Newborn	12[c]	6 (50%)	3 (25%)	3 (25%)
C57BL/6–129/SvJ	Het/Het	Weaning	198[d]	65 (33%)	97 (49%)	36 (18%)

[a]Out of seven pups: 3 dead and 3 dying right after birth

[b]Out of three litters of newborn pups: 2 Het and 9 KO dead or dying right after birth

[c]Out of twelve pups: 2 WT, 1 Het and 3 KO dead or dying right after birth

[d]Published in Maccarana et al., 2009

multiple comparison test. Error bars are SEM if not stated otherwise in the figure text.

Results

GENERATION OF *DSE* KO MICE IN PURE C57BL/6 AND NFR GENETIC BACKGROUNDS

Different genetic backgrounds may generate diverse phenotypes for the same genetic mutation (Montagutelli, 2000).

This is also the case for DS-epi1-deficient mice. In mixed C57BL/6–129/SvJ genetic background, the KO mice were viable and presented at the expected Mendelian frequency (Table 1) and could be characterized as adults (Maccarana et al., 2009). These mice were backcrossed with mice of either C57BL/6 or NFR genetic background for more than 10 generations. In the C57BL/6 genetic background, all *Dse* KO mice died perinatally (Table 1), while at E14.5/E15.5 they were present at the expected Mendelian frequency. In the current study the major focus was on mice in the NFR genetic background in which 155 embryos in total were analyzed. We demonstrated that in the mixed C57BL/6–129/SvJ genetic background, *Dse* Het mice had approximately half the amount of the DS-epi1 enzyme compared with WT littermates. Despite this fact, the amount, the length and the structure of CS/DS chains were identical in *Dse* Het mice compared with WT littermates (Maccarana et al., 2009). Therefore, to achieve the highest numbers of *Dse* KO embryos for developmental studies, *Dse* Het mice were generally mated with *Dse* KO mice. The resulting offspring had a Mendelian distribution between *Dse* Het and *Dse* KO genotypes. Approximately 70% (12 of 17 newborn pups from 4 litters) of the *Dse* KO pups were dead or dying at birth (Table 1).

DEVELOPMENTAL DEFECTS IN *DSE* KO EMBRYOS IN PURE NFR GENETIC BACKGROUND

Previously we reported a 20 to 30% reduction of body weight in *Dse* KO mice compared with their WT littermates in mixed C57BL/6–129/SvJ genetic background (Maccarana et al., 2009). Analysis of *Dse* KO embryos and *Dse* Het littermates in the NFR genetic background showed similar body weights during embryonic development and a marginal decrease (6%) at birth ($p = 0.27$; Suppl. Fig. 1) (which is available online).

All *Dse* KO embryos in pure NFR genetic background had kinked tails (Fig. 1A′, black arrow; Table 2), similar to *Dse* KO embryos in the mixed C57BL/6–129/SvJ genetic background. Twenty-one percent of the *Dse* KO embryos showed other severe developmental defects (Table 2). The dominating defect, seen in 16% of the *Dse* KO embryos, was an abdominal wall defect (AWD) with herniated intestines (Fig. 1A′, 1B′, and C, empty arrowheads; Table 2). During normal mouse development from approximately E12.5, loops of the midgut protrude through the abdominal wall at the umbilicus, a phenomenon denoted as physiological umbilical hernia. By E15.5, retraction of the intestines into the peritoneal cavity begins and by E16.5 the ventral body wall closes (Brewer and Williams, 2004a). In the *Dse* Het embryos the physiological umbilical hernia has been fully resolved by E16.5. In the *Dse* KO embryos, however, herniated intestines were seen outside of the ventral body wall together with remnants of a thin membrane (Fig. 1B′ and Suppl. Fig. 2, black arrows). There was no apparent difference in the size of the umbilical ring between *Dse* KO and *Dse* Het, and the appearance of the umbilical cord was similar. Other defects observed in 5% of the *Dse* KO mice were: exencephaly (Fig. 1D), spina bifida, and ringelschwanz (Kokubu et al., 2004) (Table 2). None of the *Dse* WT or Het embryos had detectable developmental defects.

THICKER EPIDERMIS IN *DSE* KO EMBRYOS AND NEWBORN MICE

Embryos at E13.5, E16.5, and E18.5, and tails from newborn pups, were paraffin embedded and sectioned. The skin surface of *Dse* KO pups appeared similar to that of their *Dse* Het littermates. Upon histological examination, however, *Dse* KO skin revealed a thickening of the epidermis. The thickness of the epidermal layers from stratum

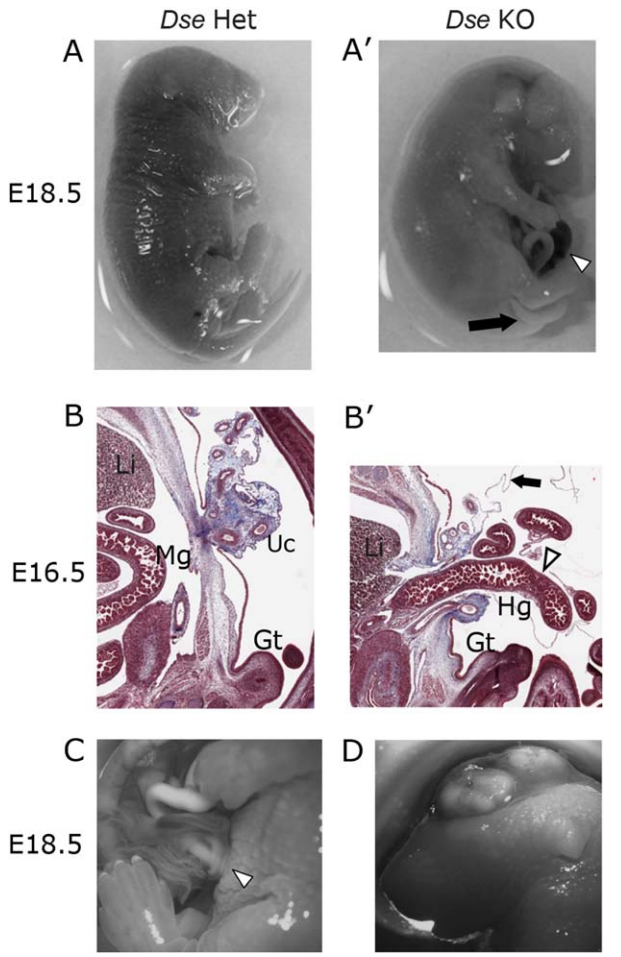

FIGURE 1. *Representative images on Dse KO embryos with embryological defects: kinked tail, AWD, and exencephaly.* **A:** *Dse Het and* **(A′)** *Dse KO embryo at E18.5 with kinked tail (black arrow) and AWD (empty arrowhead).* **B:** *Masson's trichrome staining of sagittal sections on E16.5 Dse Het embryo showing the closed ventral body wall with only the umbilical cord outside of the body, while* **(B′)** *Dse KO embryo shows AWD with part of the midgut (empty arrowhead) outside of the body, close to the umbilical cord and surrounded by remnants of a thin membrane (black arrow).* **C:** *Magnification of the abdominal area in an E18.5 Dse KO embryo showing intestinal herniation through the umbilical ring (empty arrowhead).* **D:** *Exencephaly was observed in one Dse KO embryo (E18.5). Abbreviations: Gt, genital tubercle; Hg, herniated gut; Li, liver; Mg, midgut; Uc, umbilical cord.*

basale to stratum corneum was measured around the whole body of the embryos and on the newborn tails. Morphometric measurements indicated that *Dse* KO embryos had approximately 27% thicker epidermal layer compared with *Dse* Het littermates over time from E13.5 to E18.5 ($p = 0.019$) (Fig. 2A). In addition, measurements of newborn tail epidermis indicated that *Dse* KO had 21% thicker epidermal layer compared with *Dse* WT and 17% thicker epidermal layer compared with *Dse* Het littermates ($p < 0.01$) (Fig. 2B).

ALTERATIONS IN THE EPIDERMAL LAYERS IN *DSE* KO MICE

One explanation for increased epidermal thickness in *Dse* KO mice could be defective differentiation of the keratinocytes in the epidermal layers (Byrne et al., 1994; Fuchs and Raghavan, 2002).

To study this, we used keratin 5, a marker for immature keratinocytes in the epidermal basal layer (stratum basale), which showed stronger staining intensity in tail sections from newborn *Dse* KO than in WT and *Dse* Het pups at the basal layer (Fig. 3A). In addition, Western blot analysis of whole skin extracts from WT, *Dse* Het, and *Dse* KO newborn pups showed approximately a 1.6-fold increase in keratin 5 expression in *Dse* KO skin compared with WT skin (Fig. 3B). Thickening of the epidermal layer could also depend on expanding epidermal spinous layer (stratum spinosum). Indeed, staining for the spinous layer marker, keratin 1, showed more intense immunoreactivity in newborn tail sections from *Dse* KO pups than in WT and *Dse* Het pups (Fig. 3A). However, there were no significant differences in the expression of keratin 1 assessed by Western blot analysis from whole skin extracts between the genotypes (not shown). Staining for loricrin, which is a marker for the granule cell layer (stratum granulosum), did not indicate any increased expression in *Dse* KO compared with WT or *Dse* Het pups (Fig. 3A). In addition, immunolabeling for Ki67 showed slightly decreased proliferation in *Dse* Het and KO epidermal basal layer compared with WT littermates; however the difference between the genotypes was not significant (Suppl. Fig. 3).

Discussion

In the present work, we studied the embryonic and newborn phenotype of KO mice deficient in the enzyme DS-epi1 in pure NFR background. Beside the AWD and neural tube defects (NTDs), the cause of death in the rest of the pups was possibly due to respiratory or circulatory failure, because some of the live-born *Dse* KO pups that died turned cyanotic soon after birth. Similar observations were made in the few live-born pups in the pure C57BL/6 genetic background. Respiratory failure was probably also a cause of death in mice with targeted mutations for heparan sulfate (HS) biosynthetic enzymes such as *Ndst1*

TABLE 2. *Phenotypes in NFR genetic background*

Genotype	Kinked tail	Herniated gut	Other defects: Exencephaly; Spina bifida; Ringelschwanz
Dse WT	0	0	0
Dse Het	0	0	0
Dse KO	77 (100%)	12 (16%)[a]	4 (5%)[a]

[a]Percentage out of total seventy-seven KO embryos and pups

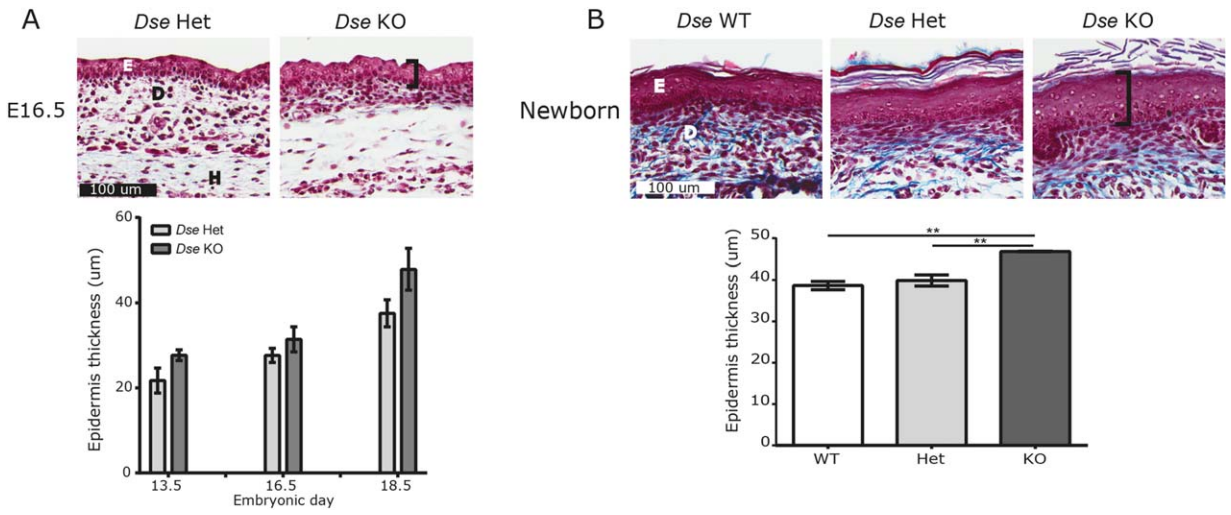

FIGURE 2. *Dse KO embryos and newborns have thicker epidermis.* **A:** *Representative images on latero-sagittal sectioned* **Dse** *Het and KO embryos at E16.5. Morphometric measurements on the epidermal layer from E13.5 to E18.5 indicated increased thickness over time with a significant difference between the genotypes ($p = 0.019$) with an average of 4.95 μm (27%) thicker layer (95% CI, 1.09–10.61) in* **Dse** *KO than in* **Dse** *Het littermates.* **B:** *Representative images on transversely sectioned tails from WT,* **Dse** *Het and KO newborn pups. Morphometric measurements indicated a significantly thicker epidermal layer in* **Dse** *KO mice than in WT (8.11 μm, 95% CI, 3.93–12.3) and in* **Dse** *Het littermates (6.9 μm, 95% CI, 2.71–11.1), respectively (Scale bars = 100 μm). Brackets in* **Dse** *KO images indicate the epidermal layer (from stratum basale to stratum corneum). Abbreviations: E, epidermis; D, dermis; H, hypodermis. Morphometric measurements were analyzed by two-way ANOVA (embryonic epidermis) or Student's t test and one-way ANOVA (newborn tail). **indicates $p < 0.01$. Error bars are SEM.*

(Ringvall and Kjellen, 2010) and the epimerase *Glce* (Li et al., 2003). It is a common finding that a more severe phenotype due to gene ablation is seen in mice with a pure genetic background, such as in both C57BL/6 and NFR mouse models, than in mice with a mixed genetic background.

ABDOMINAL WALL DEFECT IN *DSE* KO MICE

The dominating developmental defect in *Dse* KO mice in pure NFR background is an AWD with herniated intestines, noted in 16% of the embryos and newborn pups. Recent findings indicate herniation of the intestines in some of the *Dse/Dsel* double KO embryos from the mixed C57BL/6–129/SvJ genetic background (unpublished observations, X. Stachtea).

In humans, the two major AWDs are omphalocele (OC) and gastroschisis (GS), with a combined incidence of approximately 6/10.000 live births (Prefumo and Izzi, 2014). Although similar in many aspects, they show important differences regarding appearance, etiology, comorbidity and prognosis (Prefumo and Izzi, 2014).

OC is the result of an enlarged umbilical ring, allowing parts of the abdominal contents to herniate to the outside of the abdominal cavity. The extra-abdominal organs are covered by peritoneum and by the amnion membrane continuous with the umbilical cord, while the protruded contents are located at the base of the cord. Being strongly associated with other congenital defects and syndromes, the etiology of OC is considered to be mainly genetic. In contrast, in GS, no hernial sac is present, and the defect is located outside of the umbilical ring, typically on the right side. The appearance of the umbilicus (ring and cord) is normal. Although generally thought to be a result of environmental factors, familial GS does occur, and the estimated familial recurrence risk of 2.4 to 4.7% (Torfs and Curry, 1993; Kohl et al., 2010), indicates that there is a genetic contribution in some cases.

In a few KO mouse models, the AWDs have been classified and/or described as GS. However, it is hard to compare the different suggested models of GS because the described features are very diverse (Carnaghan et al., 2013). Phenotypically, most of the existing mouse models seem to be a mixture of OC and GS, including mice deficient in *Scrib* (Carnaghan et al., 2013; Murdoch et al., 2003), *Aebp1* (Layne et al., 2001; Danzer et al., 2010), *Bmp1* (Suzuki et al., 1996), and *Tfap2a* (Brewer and Williams, 2004b) (description summarized in Table 3). Our mouse model also showed features of both conditions, but the location of the defect was that of an OC. However, the defect seemed to be separated from the umbilical cord, which had a normal appearance, in concordance with GS. Similarly, the umbilical ring did not seem to be enlarged. On the contrary, although no intestines were seen to have a covering membrane, remnants of a thin membrane at the base of the extra-abdominal contents gave the impression that there had been a previous cover, thus resembling an OC.

Although all these "GS" mouse models, including ours, have several characteristics in common with human GS, it

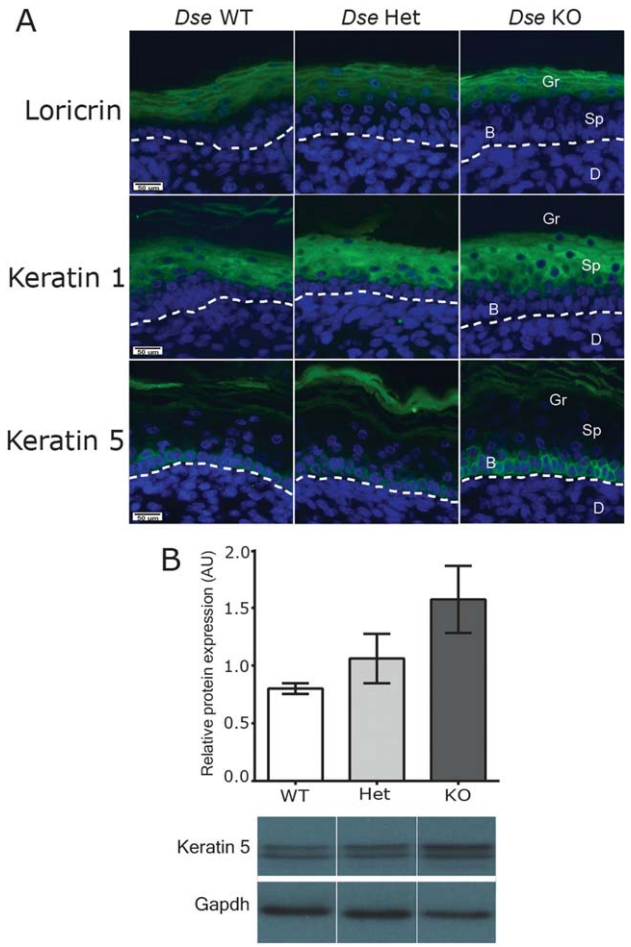

FIGURE 3. *Expression of the epidermal layer markers in WT, Dse Het, and KO epidermis.* **A:** *Immunohistochemical staining of transversally sectioned newborn tails from WT, Dse Het and Dse KO mice for loricrin, keratin1 and keratin 5 (green) and Dapi (blue). Note enhanced keratin 1 staining in the spinous layer and keratin 5 staining in the basal layer in Dse KO epidermis compared with WT and Dse Het epidermis (n=3 for each genotype). Dotted line denotes the dermo–epidermal border. Abbreviations: Gr, granular layer; Sp, spinous layer; B, basal layer; D, dermis. (Scale bars = 50 μm).* **B:** *Densitometric analysis and representative western blot images of keratin 5 on whole body skin extracts from newborn WT, Dse Het and Dse KO mice (n = 3 for each genotype). There was a 1.6-fold increase in keratin 5 expression in Dse KO skin compared with WT skin. Gapdh was used as internal loading control. Gel images were analyzed in ImageJ program, and statistical differences were calculated by one-way ANOVA. AU, arbitrary units. Error bars are SEM.*

has yet to be established whether they suffice as model systems for the defect. In none of the models has the defect been described as located outside of the umbilical ring, which constitutes a major difference to that of the human phenotype. Information about the umbilical ring size and cord appearance is often incomplete in the reports. Also, in general, there are uncertainties regarding the comparability of the ventral abdominal wall development between the two species. It is known that the location of the yolk sac differs between mice and humans, and this structure could play an important role in the pathogenesis of GS (Feldkamp et al., 2007; Stevenson et al., 2009).

The pathogenesis of the AWD in our model is uncertain, but given the collagen phenotype in the *Dse* KO skin (Maccarana et al., 2009), IdoA content could play an important role for proper collagen maturation and closure of the ventral body during embryogenesis. This is supported by the notion that mice deficient in BMP-1, a matrix metalloproteinase processing the C-terminal propeptide of fibrillar pro-collagens I, II and III, also develop an AWD (Suzuki et al., 1996). Furthermore, failure of ventral body closure could be ascribed to lack of FGFR1 and FGFR2 signaling, because conditionally mutated *Fgfr1/Fgfr2* mice exhibit disruption in the secondary abdominal wall patterning closest to the skin and ventral midline, resulting in OC (Nichol et al., 2011).

Further research is needed regarding normal development of the abdominal wall in mice and humans as well as the pathogenesis of different AWDs.

NEURAL TUBE DEFECTS IN *DSE* KO MICE

In the present study, 5% of the *Dse* KO mice exhibited exencephaly or spina bifida, i.e., NTDs. The equivalent of exencephaly in humans is called anencephaly, in which the child is born without the major part of the brain (the exencephaly evolves into anencephaly because the brain is degenerated upon exposure to the amniotic fluid). The causes of NTDs are multifactorial and probably depend on both genetic and environmental factors (Copp et al., 2013). Exencephaly results from failure to close the cranial portion of the neural tube in early development during the primary neurulation (Wallingford et al., 2013), whereas spina bifida results from a more distal closure failure. Deficiencies in several genes have been shown to cause these malformations, and there are several mouse models (Harris and Juriloff, 2010). The penetrance is varying depending both on the gene and the mouse strain. For example in mice deficient in *Splotch*, the penetrance of the exencephaly phenotype was almost 80 % in one background and only 40% in another (Fleming and Copp, 2000). This can explain why no pups with exencephaly were seen in *Dse* KO mice from the mixed C57BL/6–129/SvJ genetic background (Maccarana et al., 2009).

THICKER EPIDERMAL LAYERS IN *DSE* KO MICE

The present study demonstrates the importance of IdoA content in DS-PGs during epidermal morphogenesis, because histological staining indicates a thickening of the epidermis in *Dse* KO embryos and newborn pups.

Both the epidermis and the neural tube derive from the ectoderm. The neural tube is formed from the neural plate that consists of a thickened ectoderm, separated from the epidermis at the neural plate borders. The neural plate borders serve as the adjoining points when the

TABLE 3. *Comparison of mouse KO models with abdominal wall defects with human gastroschisis (GS) and omphalocele (OC).*

	Exact location	Umbilical Ring (UR)	Umbilical Cord (UC)	Covering	Protruded organs	Penetrance	Gene analysis in human GS-patients	References
				Human defect				
GS	To the right of umbilicus	Normal	Normal appearance, separated from the defect	No	Bowel and occationally other organs			
OC	UR	Enlarged	Hernia in the base of UC	Yes (peritoneum and amnion membrane)	Bowel and occationally other organs			
				Mouse model				
Aebp1	Adjacent to the umbilicus	NA*	NA	No	Bowel, liver	100%	No disease-causing mutations in 40 patients	Layne et al, 2001; Danzer et al. 2010; Feldkamp et al, 2012
Tfap-2a	UR	Enlarged	NA	No	Bowel, liver	NA		Brewer and Williams, 2004
Bmp1	NA	NA	NA	No	Bowel	78–84%	No mutations in 11 patients	Suzuki et al. 1996; Komuro et al, 2001
Scrib (2 different types of AWDs)	UR	Enlarged	Hernia in the base of UC	Yes	Bowel, liver			Camaghan et al, 2013
	Complete failure of ventral abdominal wall closure		Normal appearance, membrane in continuation with that of UC	Yes (only thin, ruptured membrane)	Bowel, liver, stomach, spleen	23% in total (both AWDs)		
Dse	UR	Normal appearance	Normal appearance, separated from the defect	Yes (only thin, ruptured membrane)	Bowel	16%		(present study)

The table shows the comparison of six KO models of AWD with specific clinical and developmental features of the most common human AWDs, GS and OC respectively. *NA = non applicable

neural tube closes (Aybar et al., 2002). Given this joint origin, the thickened epidermis and the NTDs might have a common mechanism in our mouse model.

One of the functions of CS/DS-PGs is to bind and store growth factors. During development of the neural plate border, a cascade of signaling events orchestrated by growth factors (e.g., FGFs, EGFs) and morphogens (e.g., WNTs) takes place (Groves and LaBonne, 2014). Highly sulfated GAGs such as HS and DS are crucial for these signaling pathways (Niehrs, 2012). Deletion of *Ndst1* not only causes respiratory failure (Ringvall and Kjellen, 2010), but also NTDs (exencephaly and spina bifida) at a similar penetrance as ours (6%) in one model (Pallerla et al., 2007). It is possible that there is a partial redundancy between DS and HS in these signaling pathways, which could explain the relatively low penetrance of these phenotypes.

Transcription factor AP-2α (*Tfap2a*) induces the expression of several epidermally related genes (Byrne et al., 1994). Mice deficient in *Tfap2a* exhibited severe ventral body wall defects (Brewer and Williams, 2004b) and had elevated expression levels of EGF receptor in the epidermis (Wang et al., 2006). However, these mice showed increased cell proliferation in the basal layer of the epidermis, which is opposite to the slightly decreased proliferation observed in *Dse* KO epidermal basal layer.

The epidermal thickening in *Dse* KO mice correlated with an increased staining for the basal layer marker, keratin 5, and the spinous layer marker, keratin 1. Of interest, expression of dominant-negative FGFR in mice resulted in thickened epidermal layers and an increased expression of keratin 14 in the basal epidermal layer (Werner et al., 1993). Keratinocyte growth factor (KGF or FGF-7), FGF2 and FGF10 have been shown to preferentially bind to IdoA-containing motifs in CS/DS-PGs, promoting proliferative processes during wound healing (Taylor et al., 2005; Plichta and Radek, 2012). It is tempting to speculate that lower IdoA content in the dermal and epidermal interstitium may affect FGF-signaling leading to the different phenotypes observed in *Dse* KO mice. Paracrine signals from fibroblasts in the dermis toward the keratinocytes in the epidermis may be delayed as a result of lowered binding capacity for growth factors in *Dse* KO skin.

Furthermore, decorin deficient mice have higher amounts of CS/DS in the skin, but with less charge, similar to the structure of DS produced in the *Dse* KO mice in mixed C57BL/6–129/SvJ genetic background (Maccarana et al., 2009; Nikolovska et al., 2014). Highly-sulfated GAGs from decorin deficient fibroblast and keratinocytes co-cultured in 3D-condition caused a delayed keratinocyte differentiation (Nikolovska et al. 2014), a finding that could be applied on the *Dse* KO epidermal phenotype, because proliferation in the epidermal basal layer, assessed by Ki67 staining, was somewhat lower in *Dse* KO compared with WT skin.

In conclusion, DS-epi1 deficiency in pure NFR mice generated several developmental malformations, with AWD being the dominant defect. In addition, *Dse* KO mice had thicker epidermal layers and an increased expression of the epidermal basal and spinous layer markers. With regard to the increasing tendency of various AWDs in neonates worldwide, our *Dse* null mice could serve as a model for human AWDs. In addition, this model could be a useful tool in search for etiological and pathogenetical mechanisms causing AWDs.

Acknowledgments

Statistical support from Susann Ullén is greatly appreciated. The authors have no conflict of interest to declare.

References

Aybar MJ, Glavic A, Mayor R. 2002. Extracellular signals, cell interactions and transcription factors involved in the induction of the neural crest cells. Biol Res 35:267–275.

Bartolini B, Thelin MA, Rauch U, et al. 2012. Mouse development is not obviously affected by the absence of dermatan sulfate epimerase 2 in spite of a modified brain dermatan sulfate composition. Glycobiology 22:1007–1016.

Brewer S, Williams T. 2004a. Finally, a sense of closure? Animal models of human ventral body wall defects. Bioessays 26:1307–1321.

Brewer S, Williams T. 2004b. Loss of AP-2alpha impacts multiple aspects of ventral body wall development and closure. Dev Biol 267:399–417.

Bulow HE, Hobert O. 2006. The molecular diversity of glycosaminoglycans shapes animal development. ANNU REV CELL DEV BIOL 22:375–407.

Byrne C, Tainsky M, Fuchs E. 1994. Programming gene expression in developing epidermis. Development 120:2369–2383.

Carnaghan H, Roberts T, Savery D, et al. 2013. Novel exomphalos genetic mouse model: the importance of accurate phenotypic classification. J Pediatr Surg 48:2036–2042.

Copp AJ, Stanier P, Greene ND. 2013. Neural tube defects: recent advances, unsolved questions, and controversies. Lancet Neurol 12:799–810.

Danzer E, Layne MD, Auber F, et al. 2010. Gastroschisis in mice lacking aortic carboxypeptidase-like protein is associated with a defect in neuromuscular development of the eviscerated intestine. Pediatr Res 68:23–28.

Esko JD, Kimata K, Lindahl U. 2009. Proteoglycans and sulfated glycosaminoglycans. In: Varki A, Cummings RD, Esko JD, Freeze HH, Stanley P, Bertozzi CR, Hart GW, Etzler ME, editors. Essentials of glycobiology. 2nd ed. New York: Cold Spring Harbor.

Feldkamp ML, Carey JC, Sadler TW. 2007. Development of gastroschisis: review of hypotheses, a novel hypothesis, and implications for research. Am J Med Genet Part A 143:639–652.

Fleming A, Copp AJ. 2000. A genetic risk factor for mouse neural tube defects: defining the embryonic basis. Hum Mol Genet 9: 575–581.

Fuchs E, Raghavan S. 2002. Getting under the skin of epidermal morphogenesis. Nat Rev Genet 3:199–209.

Groves AK, LaBonne C. 2014. Setting appropriate boundaries: fate, patterning and competence at the neural plate border. Dev Biol 389:2–12.

Harris MJ, Juriloff DM. 2010. An update to the list of mouse mutants with neural tube closure defects and advances toward a complete genetic perspective of neural tube closure. Birth Defects Res Part A Clin Mol Teratol 88:653–669.

Kohl M, Wiesel A, Schier F. 2010. Familial recurrence of gastroschisis: literature review and data from the population-based birth registry "Mainz Model". J Pediatr Surg 45:1907–1912.

Kokubu C, Heinzmann U, Kokubu T, et al. 2004. Skeletal defects in ringelschwanz mutant mice reveal that Lrp6 is required for proper somitogenesis and osteogenesis. Development 131:5469–5480.

Layne MD, Yet SF, Maemura K, et al. 2001. Impaired abdominal wall development and deficient wound healing in mice lacking aortic carboxypeptidase-like protein. Mol Cell Biol 21:5256–5261.

Li JP, Gong F, Hagner-McWhirter A, et al. 2003. Targeted disruption of a murine glucuronyl C5-epimerase gene results in heparan sulfate lacking L-iduronic acid and in neonatal lethality. J Biol Chem 278:28363–28366.

Liljander M, Andersson A, Holmdahl R, Mattsson R. 2009. Increased litter size and super-ovulation rate in congenic C57BL mice carrying a polymorphic fragment of NFR/N origin at the Fecq4 locus of chromosome 9. Genet Res (Camb) 91: 259–265.

Maccarana M, Kalamajski S, Kongsgaard M, et al. 2009. Dermatan sulfate epimerase 1-deficient mice have reduced content and changed distribution of iduronic acids in dermatan sulfate and an altered collagen structure in skin. Mol Cell Biol 29:5517–5528.

Malmstrom A, Bartolini B, Thelin MA, et al. 2012. Iduronic acid in chondroitin/dermatan sulfate: biosynthesis and biological function. J Histochem Cytochem 60:916–925.

Miyake N, Kosho T, Mizumoto S, et al. 2010. Loss-of-function mutations of CHST14 in a new type of Ehlers-Danlos syndrome. Hum Mutat 31:966–974.

Montagutelli X. 2000. Effect of the genetic background on the phenotype of mouse mutations. J Am Soc Nephrol 11(Suppl 16): S101–S105.

Muller T, Mizumoto S, Suresh I, et al. 2013. Loss of dermatan sulfate epimerase (DSE) function results in musculocontractural Ehlers-Danlos syndrome. Hum Mol Genet 22:3761–3772.

Murdoch JN, Henderson DJ, Doudney K, et al. 2003. Disruption of scribble (Scrb1) causes severe neural tube defects in the circletail mouse. Hum Mol Genet 12:87–98.

Nichol PF, Corliss RF, Tyrrell JD, et al. 2011. Conditional mutation of fibroblast growth factor receptors 1 and 2 results in an omphalocele in mice associated with disruptions in ventral body wall muscle formation. J Pediatr Surg 46:90–96.

Niehrs C. 2012. The complex world of WNT receptor signalling. Nat Rev Mol Cell Biol 13:767–779.

Nikolovska K, Renke JK, Jungmann O, et al. 2014. A decorin-deficient matrix affects skin chondroitin/dermatan sulfate levels and keratinocyte function. Matrix Biol 35:91–102.

Pallerla SR, Pan Y, Zhang X, et al. 2007. Heparan sulfate Ndst1 gene function variably regulates multiple signaling pathways during mouse development. Dev Dyn 236:556–563.

Plichta JK, Radek KA. 2012. Sugar-coating wound repair: a review of FGF-10 and dermatan sulfate in wound healing and their potential application in burn wounds. J Burn Care Res 33:299–310.

Prefumo F, Izzi C. 2014. Fetal abdominal wall defects. Best Pract Res Clin Obstet Gynaecol 28:391–402.

Ringvall M, Kjellen L. 2010. Mice deficient in heparan sulfate N-deacetylase/N-sulfotransferase 1. Prog Mol Biol Transl Sci 93:35–58.

Stevenson RE, Rogers RC, Chandler JC, et al. 2009. Escape of the yolk sac: a hypothesis to explain the embryogenesis of gastroschisis. Clin Genet 75:326–333.

Suzuki N, Labosky PA, Furuta Y, et al. 1996. Failure of ventral body wall closure in mouse embryos lacking a procollagen C-proteinase encoded by Bmp1, a mammalian gene related to Drosophila tolloid. Development 122:3587–3595.

Taylor KR, Rudisill JA, Gallo RL. 2005. Structural and sequence motifs in dermatan sulfate for promoting fibroblast growth factor-2 (FGF-2) and FGF-7 activity. J Biol Chem 280:5300–5306.

Thelin MA, Bartolini B, Axelsson J, et al. 2013. Biological functions of iduronic acid in chondroitin/dermatan sulfate. FEBS J 280:2431–2446.

Torfs CP, Curry CJ. 1993. Familial cases of gastroschisis in a population-based registry. Am J Med Genet 45:465–467.

Wallingford JB, Niswander LA, Shaw GM, Finnell RH. 2013. The continuing challenge of understanding, preventing, and treating neural tube defects. Science 339:1222002.

Wang X, Bolotin D, Chu DH, et al. 2006. AP-2alpha: a regulator of EGF receptor signaling and proliferation in skin epidermis. J Cell Biol 172:409–421.

Werner S, Weinberg W, Liao X, et al. 1993. Targeted expression of a dominant-negative FGF receptor mutant in the epidermis of transgenic mice reveals a role of FGF in keratinocyte organization and differentiation. EMBO J 12:2635–2643.